SIMPLE EXPRESSIONS OF CONSTRUCTING FRAGILITY CURVES FOR ISOLATED HIGHWAY BRIDGES

Kazi R. KARIM[1] and Fumio YAMAZAKI[2]

ABSTRACT: The trend of isolating highway bridges is on the rise after the recent large earthquakes in Japan, the United States, and other countries. Recent investigation shows that isolated systems perform well against seismic forces as the substructures of such systems experience less lateral forces due to energy dissipation of the isolation device. Hence, it is anticipated that there might be an effect on fragility curves of highway bridges due to isolation. In this study, thirty (30) isolated bridge models were considered to have a wider range of the variation of structural parameters, e.g., pier heights, weights, and over-strength ratio of structures. Then, fragility curves were developed by following a simplified procedure using two hundred and fifty (250) strong motion records, which were selected from five earthquake events that occurred in Japan, the USA, and Taiwan. It is observed that the level of damage probability for the isolated system is less than that of the non-isolated one for a lower level of pier height. However, having the same over-strength ratio of the structures, the level of damage probability for the isolated system is found to be higher for a higher level of pier height compared to the one of the non-isolated system.

Key Words: strong motion record, highway bridge, dynamic analysis, fragility curve

INTRODUCTION

Fragility curves are regarded to be useful tools for estimating the extent of probable damages (slight, moderate, extensive, and complete) of structures due to an earthquake (Basoz and Kiremidjian, 1997; Kircher *et al.*, 1997; Mander and Basoz, 1999; Yamazaki *et al.*, 2000). It shows the probability of structure damages as a function of ground motion indices, e.g., peak ground acceleration (*PGA*) and peak ground velocity (*PGV*). They allow estimating a damage level for a known ground motion index.

Yamazaki *et al.* (2000) developed a set of empirical fragility curves for highway bridges based on actual damage data from the 1995 Kobe earthquake. However, the type of structure, structural performance (static and dynamic) and variation of input ground motions were not considered in the empirical approach. It is assumed that structural parameters and input motion characteristics (e.g., frequency contents, phase, and duration) have influence to the damage of structures for which there will be an effect on fragility curves.

The present authors (Karim and Yamazaki, 2001) developed a set of analytical fragility curves for highway bridge piers based on numerical simulation considering the variation of input ground motions. It was found that there is a significant effect of earthquake ground motions on fragility curves. They also developed a simplified method (Karim and Yamazaki, 2003) to construct the fragility curves of non-isolated highway bridges considering the variation of both input ground motions and structural

[1] Postdoctoral Fellow
[2] Associate Professor

parameters. It was also found that there is a significant effect of both earthquake ground motions and structural parameters on fragility curves.

The trend of isolating highway bridges is on the rise after the recent damaging earthquakes in Japan, the United States, and other countries. Recent investigation shows that isolated systems perform well against seismic forces as the substructures of such systems experience less lateral forces due to energy dissipation of the isolation device (Chaudhary *et al.*, 2000). Hence, it is anticipated that there might be an effect on fragility curves of highway bridges due to isolation; in other words, fragility curves for non-isolated bridges may not be applicable to predict the extent of probable damages for isolated systems since the fragility curves of the two systems might be different.

The purpose of this study is to develop fragility curves for isolated bridges by following a simplified procedure, and to compare them with the ones of the non-isolated systems. In this objective, thirty (30) isolated bridge models are considered to have a wider range of the variation of structural parameters, e.g., pier heights, weights, and over-strength ratio of structures. A total of two hundred and fifty (250) strong motion records are considered as the input motions, which were selected from five earthquake events that occurred in Japan, the USA, and Taiwan. Then, using the selected input motions and isolated bridge models, fragility curves are obtained with respect to ground motion parameters by following a simplified approach (Karim and Yamazaki, 2003).

DEVELOPMENT OF FRAGILITY CURVES

Empirical fragility curves

Yamazaki *et al.* (2000) developed a set of empirical fragility curves based on actual damage data from the 1995 Kobe earthquake, and showed the relationship between the damages occurred to the expressway bridge structures and the ground motion indices. In this approach, the damage data of the expressway structures due to the Kobe earthquake were collected, and the ground motion indices along the expressways were estimated based on the estimated strong motion distribution using Kriging technique. The damage data and ground motion indices were related to each damage rank, and the damage ratio for each damage rank was obtained. Finally, using the damage ratio for each damage rank, the empirical fragility curves for the expressway bridge structures were constructed assuming a lognormal distribution (Sucuoglu *et al.*, 1999; Yamazaki *et al.*, 2000).

Analytical fragility curves

The present authors (Karim and Yamazaki, 2001) developed a set of analytical fragility curves for highway bridge piers based on numerical simulation and considering the variation of input ground motions. The procedures adopted to construct the analytical fragility curves are briefly described below.

In this approach, first, the nonlinear static pushover analysis of the structure is performed (Bentz and Collins, 2000; SAP2000, 2000), which includes the shear vs. strain and moment vs. curvature analyses of the cross-sections (it is recommended in the code (Design Specification of Highway Bridges, 1998) that a pier should be divided at least into 50 slices), and the force-displacement relationship at the top of the bridge pier is obtained by using the shear vs. strain and moment vs. curvature relationships of all cross-sections. Using the elastic stiffness (obtained from the force-displacement relationship), the nonlinear dynamic response analyses (Chopra, 1995) are performed for the selected input ground motions, which are normalized to different excitation levels.

The damage to the structure (pier) is then quantified by a damage index *DI* that is obtained by using a damage model (Park and Ang, 1985) and the number of occurrence of a particular damage rank is counted by calibrating (Ghobarah *et al.*, 1997) the damage indices in different excitation levels, which is used to obtain the damage ratio of each damage rank in each excitation level. The damage ratio is then plotted on a lognormal probability paper (Karim and Yamazaki, 2001; Yamazaki *et al.*, 2000) from where the two parameters of the fragility curves, i.e., mean and standard deviation are obtained by performing a linear regression analysis. Finally, fragility curves are constructed for each damage

rank with respect to the ground motion indices using the obtained mean and standard deviation. The procedures adopted for constructing the analytical fragility curves can be summarized as follows:

1. Selection of the earthquake ground motion records.
2. Normalization of *PGA* of the selected records to different excitation levels.
3. Making a physical model of the structure.
4. Performing a nonlinear static pushover analysis and obtaining the elastic stiffness of the structure.
5. Selection of a hysteretic model for the nonlinear dynamic response analysis.
6. Performing the nonlinear dynamic response analysis using the elastic stiffness and the selected records.
7. Obtaining the damage indices of the structure in each excitation level using a damage model.
8. Calibration of the damage indices for each damage rank to obtain the damage ratio in each excitation level.
9. Plotting the damage ratio in each excitation level on a lognormal probability paper and obtaining the mean and standard deviation of the fragility curves for each damage rank by performing a linear regression analysis.
10. Construction of fragility curves using the obtained mean and standard deviation with respect to the ground motion indices for each damage rank assuming a lognormal distribution.

Simplified approach to develop fragility curves

The present authors (Karim and Yamazaki, 2003) also developed a simplified method to construct fragility curves for non-isolated bridges based on the observed correlation between the fragility curve parameters and structural parameters. The procedure adopted to develop the simplified expressions of fragility curves is briefly described below.

In this approach, first, the fragility curve parameters mean λ and standard deviation ξ are obtained by performing a series of both nonlinear static pushover and dynamic response analyses. Then, the relationships between mean λ and standard deviation ξ with the over-strength ratio θ (Design Specifications of Highway Bridges, 1998; Karim and Yamazaki, 2003) are obtained considering all the data points without making any subgroups. The relationships are also obtained by making the data points into some subgroups, for instance, data points for different codes, pier heights, weights, etc. It is observed that λ and θ shows higher correlation for the data points of each level of pier height. Based on this observation, λ for different levels of pier heights are obtained by fixing some θ using the relationships between λ and θ that are obtained for different levels of pier heights. Then, the relationship between λ and h is obtained using the following regression model

$$\lambda_h = b_0 + b_1 h + b_2 h^2 \tag{1}$$

where λ_h is the mean with respect to h, h is the height of the pier, and b_0, b_1 and b_2 are the regression coefficients. Like the data points for each level of pier height, it is also found that there is a strong correlation between λ and h for different θ. It is also observed that the relationships between λ and h obtained for different θ are quite parallel, which implies that knowing only one of the relationships between λ and h for a given θ, the other relationships for different θ can also be obtained knowing only some scale factors for a change of θ. In this objective, the scale factors are obtained for changing different θ for different pier heights considering the relationship between λ and h obtained for a θ equal to 1.0, and the scale factor F_θ is given as

$$F_\theta = a_0 + a_1 \Delta\theta \tag{2}$$

where F_θ is the scale factor with respect to the change of θ, $\Delta\theta$ is the change of θ given as (θ-1), and a_0 and a_1 are the regression coefficients. Although, the scale factors for different levels of pier

heights are found to be very similar, however, to minimize the error that might results for different levels of pier heights, the average scale factor obtained for different pier heights is considered (Karim and Yamazaki, 2003). Hence, the λ value can readily be obtained using **Equation (1)** for a known h, and then simply multiplying it by the scale factor F_θ of **Equation (2)** that can be obtained for a known $\Delta\theta$. In other words, the λ value can be obtained by using the following expression

$$\lambda = \lambda_h F_\theta \tag{3}$$

Substituting for λ_h and F_θ of **Equations (1)** and **(2)** into **Equation (3)** gives

$$\lambda = [b_0 + b_1 h + b_2 h^2][a_0 + a_1 \Delta\theta] \tag{4}$$

Similar procedure has also been adopted to obtain the expression for standard deviation ξ, and the expression for ξ is given as

$$\xi = [b_0 + b_1 h + b_2 h^2][a_0 + a_1 \Delta\theta] \tag{5}$$

It should be noted that the regression coefficients of **Equation (4)** are different than that of **Equation (5)**, however, same symbols are used for simplicity. It should also be noted that the expressions of fragility curve parameters mean λ and standard deviation ξ given in **Equations (4)** and **(5)**, respectively, hold true for all damage ranks, i.e., slight, moderate, extensive, and complete with respect to both *PGA* and *PGV*. Another point also be noted that to perform regression analysis and to obtain regression coefficients b_0, b_1, b_2, a_0 and a_1 of **Equations (4)** and **(5)**, fragility curve parameters mean λ and standard deviation ξ are obtained by following the same procedures given in the preceding section, i.e., "analytical fragility curves" section, which provides the foundation for developing the simplified method to obtain the expressions of fragility curve parameters (Karim and Yamazaki, 2003).

BRIDGE MODELS

Description of bridge models

In order to obtain simplified expressions of fragility curve parameters for isolated bridges, a total of thirty (30) bridge models are considered to have a wider range of the variation of structural parameters, and they are designed (Priestley *et al.*, 1996) according to the seismic design code of highway bridges (Design Specification of Highway Bridges, 1998). For the selected bridge models, the piers are considered rectangular and fixed to the base (Ghobarah and Ali, 1988), and a Lead-Rubber Bearing (LRB) is considered as the isolation device (Chaudhary *et al.*, 2000; Ghobarah and Ali, 1988; Kawashima and Shoji, 1998). The ground condition is considered as type II, the regional class is considered as A, and the standard lateral force coefficient k_{hco} is considered as type II (Design Specifications of Highway Bridges, 1998; Karim and Yamazaki, 2003).

The bridge models are divided into three categories, viz., bridges designed with different seismic codes, bridges having different pier heights, and bridges having different span lengths or weights, however, the number of spans for the all bridge models are assumed to be four. The substructures (piers) for any typical bridge model are considered to be similar, in other words, one pier model can be considered as the representative of all other piers for a particular bridge structure. This assumption is adopted to avoid a rigorous computation necessary to perform nonlinear pushover analyses for the all piers of a particular bridge model. The physical model is considered as the one shown in **Figure 1**. The substructure stiffness of the whole bridge system is given as the sum of the stiffness of all piers (Chaudhary *et al.*, 2000), and the effective stiffness of the system is calculated using the equivalent

stiffness of the pier and the equivalent stiffness of the bearing (Kawashima and Shoji, 1998).

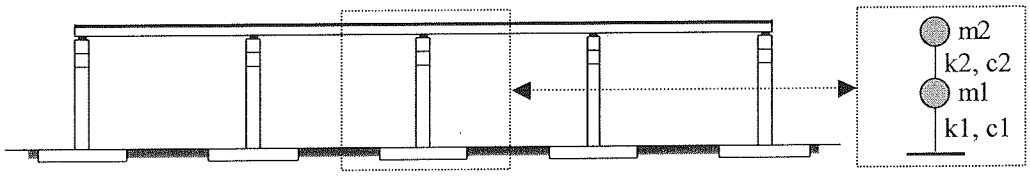

Figure 1. Physical model of an isolated bridge system used in this study

Table 1. Structural properties for the thirty (30) isolated bridge models used in this study

Design Code	Span Length, L=30m, 40m (w=500kN/m) pier height (m)										reinforcement	
	6		9		12		15		18		Long.	Tie
	section		section		section		Section		section		ρ_l (%)	ρ_t (%)
	a^1	b^2	a^1	b^2	a^1	b^2	a^1	b^2	a^1	b^2	area ratio	vol. ratio
1964	2.0	2.8	2.6	3.2	3.0	3.5	3.4	3.8	3.5	4.0	1.21	0.09
1980	2.1	3.0	2.8	3.2	3.2	3.8	3.8	4.0	3.8	4.2	1.25	0.32
1995	2.2	3.0	2.8	3.4	3.2	4.0	3.8	4.2	4.0	4.5	1.36	1.03

[1]Dimension in the longitudinal direction in m.

[2]Dimension in the transverse direction in m.

σ'_c (MPa) and σ_{sy} (MPa) are taken as the same for the all codes, and they are taken as 27 and 300, respectively.

Table 1 shows all the structural properties for different categories of bridges having span length of 30m and 40m, respectively, with superstructure weight as 500 kN/m. Note that same structural properties have been considered for the all bridge models having a span length of 40m, in other words, changing only the span length or weight of the superstructure while all other parameters being unchanged. It can be seen that the pier cross section changes for different seismic design codes even having the same height, and it changes from smaller to larger from the 1964 code to the 1995 code. It can also be seen that the pier cross section also changes due to the changes of pier height even it is designed with the same seismic code, and it changes from smaller to larger from pier height 6m to 18m. One can also see that the longitudinal (area ratio) and tie (volumetric ratio) reinforcement also changes for different seismic codes, and the value goes higher from the 1964 code to the 1995 code.

Isolation device-LRB

Kawashima and Shoji (1998) recommended that the yield force of the LRB can be taken as 10-20% weight of the superstructure (W), while Ghobarah and Ali (1988) recommended that the yield force of the LRB can be taken as 5% W, which provides a reasonable balance between reduced forces in the piers and increased forces on the abutments. However, in this study, the yield force and yield stiffness of the LRB are taken as 5% W and 5% W/mm, respectively. Given the yield force level and the lead yield strength of 10-10.5 MPa (Ghobarah and Ali, 1988; Priestley *et al.*, 1996), the number and cross sectional area of the lead plugs can be designed (Ghobarah and Ali, 1988). The advantage of LRB is that it has low yield strength and sufficiently high initial stiffness that results to higher energy

dissipation (Chaudhary *et al.*, 2000; Ghobarah and Ali, 1988; Kawashima and Shoji, 1998; Priestley *et al.*, 1996).

Elongation of natural period for isolation

The natural period T for the isolated system can be computed as (Kawashima and Shoji, 1998)

$$T = 2.01\sqrt{\frac{W}{K_e}} \tag{6}$$

where W is the weight of the superstructure and a 50% weight of the pier in kN, and K_e is the effective stiffness of the bridge in kN/m, which is given as (Kawashima and Shoji, 1998)

$$\frac{1}{K_e} = \frac{1}{K_{ep}} + \frac{1}{K_{eb}} \tag{7}$$

where T is the natural period in s, K_{ep} is the equivalent stiffness of the pier, and K_{eb} is the equivalent stiffness of the bearing, which can be evaluated as shown in **Figure 2**.

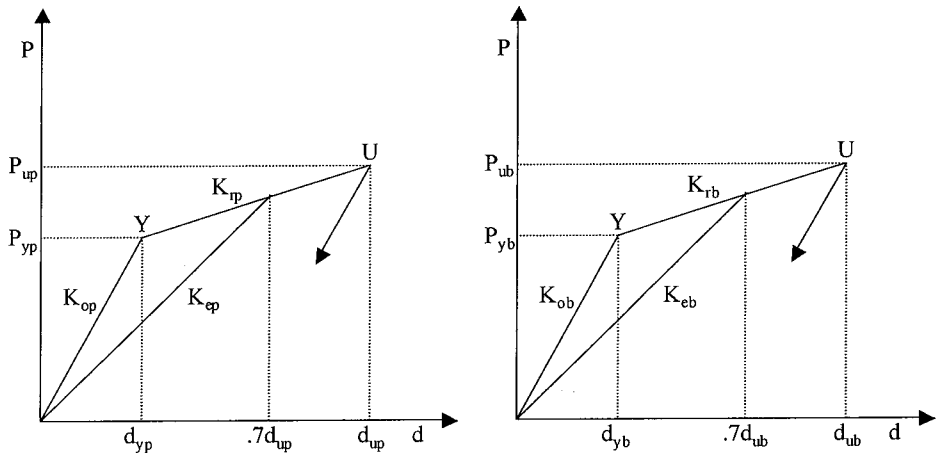

(a) Equivalent stiffness of pier (b) Equivalent stiffness of bearing

Figure 2. Definition of equivalent stiffness of the both pier and isolation device

Analytical model

For a nonlinear dynamic response analysis, the isolated bridge is modeled as a Two-Degree-of-Freedom (2DOF) system (Chaudhary *et al.*, 2000; Ghobarah and Ali, 1988; Kawashima and Shoji, 1998), a bilinear hysteretic model was considered for the both substructure (Kawashima and Macrae, 1993) and isolation device (Chaudhary *et al.*, 2000; Ghobarah and Ali, 1988; Kawashima and Shoji, 1998; Priestley *et al.*, 1996), the post-yield stiffness was taken as 10% of the initial stiffness for the both substructure and isolation device (Ghobarah and Ali, 1988; Kawashima and Shoji, 1998), the damping matrix **C** is evaluated by using the Rayleigh damping (Chopra, 1995; Priestley *et al.*, 1996), and the damping constant h_i is found by using the following expression (Design Specifications of Highway Bridges, 1998)

$$h_i = \frac{\sum_{j=1}^{n} h_j \Phi_{ij}{}^T \mathbf{K}_j \Phi_{ij}}{\Phi_i{}^T \mathbf{K} \Phi_i} \tag{8}$$

where h_j is the equivalent damping constant of element j, Φ_{ij} is the mode vector of element j of the i-th vibration mode, $\mathbf{K}_j$ is the equivalent stiffness matrix of element j, Φ_i is the mode vector of the overall structure of the i-th vibration mode, and $\mathbf{K}$ is the equivalent stiffness matrix of the overall structure.

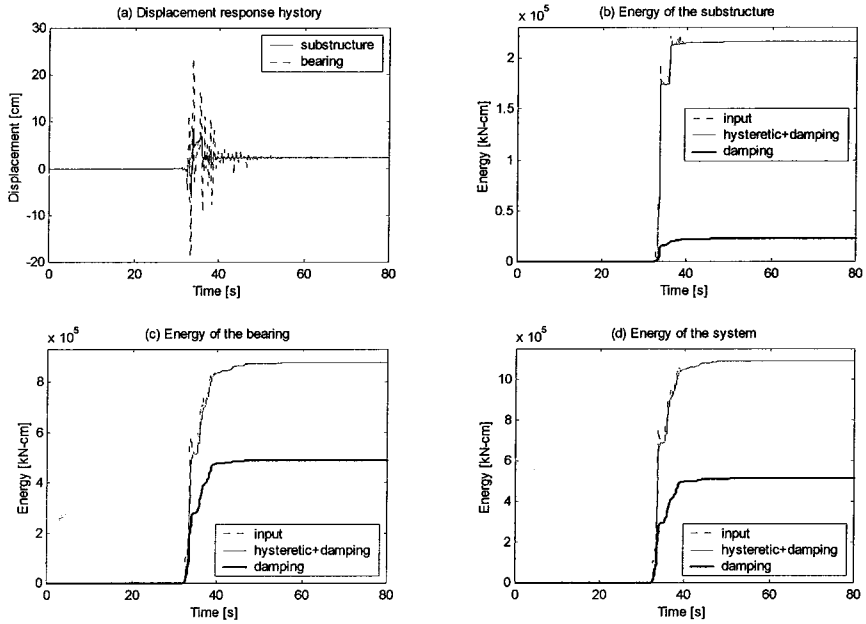

Figure 3. Displacement and energy history of an isolated bridge system obtained from the JMA Kobe NS record of the 1995 Kobe earthquake (a) displacement response history of the substructure and bearing, (b) energy of the substructure, (c) energy of the bearing, and (d) energy of the system

Displacement and energy demands

Recent investigation shows that isolated systems perform well against seismic forces as the substructures of such systems experience less lateral forces due to energy dissipation of the isolation device (Chaudhary *et al.*, 2000). Also, damage to the structure for a given input motion is related to both displacement and energy demands (Park and Ang, 1985). Hence, it is necessary to see how the displacement and energy demands of isolated systems differ from that of the non-isolated ones.

Figure 3 shows the plots of displacement and energy histories (Uang and Bertero, 1990) for the substructure and bearing of an isolated system obtained from the JMA Kobe NS record of the 1995 Kobe earthquake. It can be seen that the both displacement and energy demands of the substructure of the isolated system is less than that of the bearing. **Figure 4** shows the plots of displacement and hysteretic energy demands of the substructures for an isolated and a non-isolated system obtained from the JMA Kobe NS record. One can see that the both displacement and energy demands of the substructure of the isolated system are less than that of the substructure of the non-isolated ones. The lower level of both displacement and energy demands of the substructure of the isolated system than

that of the non-isolated ones result due to the energy dissipation of the isolation device (Chaudhary *et al.*, 2000; Ghobarah and Ali, 1988; Kawashima and Shoji, 1998), and it implies that the isolated system performs better against seismic forces than the non-isolated system does.

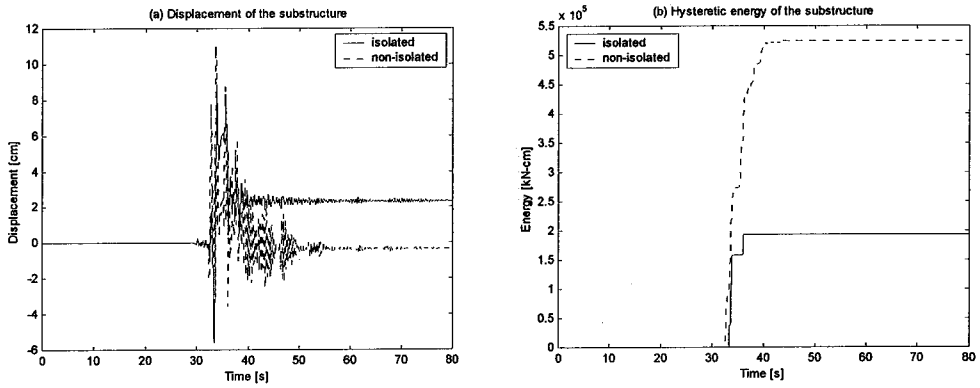

Figure 4. (a) Displacement response history, and (b) hysteretic energy of the substructures of an isolated and a non-isolated bridge system obtained from the JMA Kobe NS record of the 1995 Kobe earthquake

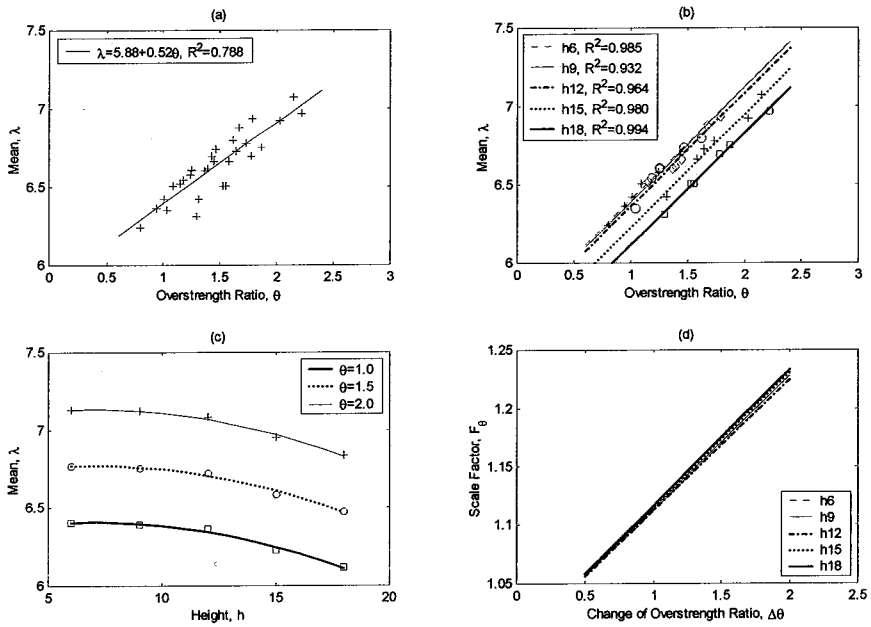

Figure 5. Relationship between (a) λ and θ obtained for the thirty isolated bridge models used in this study, (b) λ and θ for different pier heights, (c) λ and h for different θ, and (d) F_θ and $\Delta\theta$ for different pier heights, all for a slight damage with respect to *PGA*

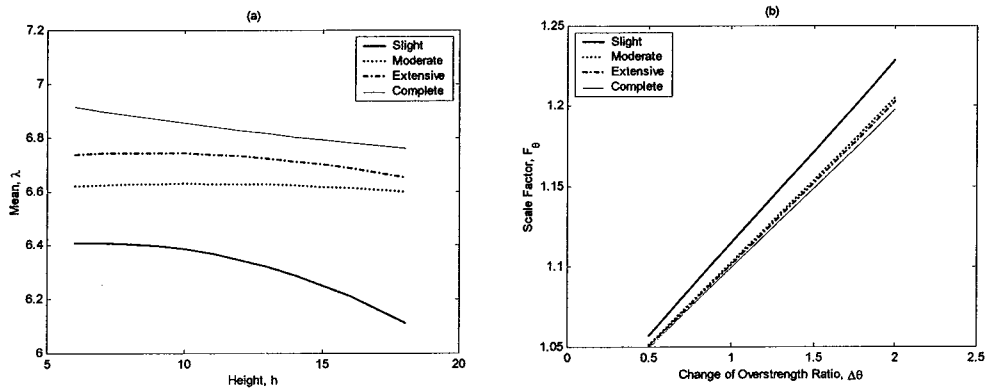

Figure 6. Relationship between (a) λ and h for a θ equal to 1.0, and (b) average F_θ and $\Delta\theta$ obtained for different damage ranks with respect to *PGA*

SIMPLIFIED EXPRESSIONS OF FRAGILIGYT CURVE PARAMETERS

Fragility curve parameters λ and ξ for the thirty (30) isolated bridge models are obtained by following the same procedure given in the "Analytical fragility curves" (Karim and Yamazaki, 2001) section using the selected two hundred and fifty (250) records as the input motions. Then, simplified expressions for the both λ and ξ of **Equations (4)** and **(5)** are obtained by following the same procedure given in the "Simplified approach to develop fragility curves" (Karim and Yamazaki, 203) section. **Figure 5** shows the graphical representation to obtain the simplified expression for λ for a slight damage with respect to *PGA*. **Figure 6(a)** shows the relationships between λ and θ obtained for different damage ranks with respect to *PGA* for a θ equal to 1.0, and the corresponding average scale factors for λ obtained for different damage ranks are shown in **Figure 6(b)**. Finally, the regression coefficients of **Equations (4)** and **(5)** are obtained for the all damage ranks with respect to both *PGA* and *PGV* by performing the both linear and nonlinear regression analyses, and the regression coefficients are shown in **Table 2**. Note that the corresponding R^2 values are also shown in the same **Table**.

Numerical example

To see how the simplified expressions of fragility curve parameters work, a different bridge structure is considered, which was not used to obtain the simplified expressions. The bridge is designed according to the recent seismic design code (Design Specifications of Highway Bridges, 1998). It is assumed that only the number of spans, span length, superstructure weight, height and cross-section of the pier can be changed while other conditions being the same as that of the thirty bridge models that were used to develop the simplified expressions. For the example bridge structure, the number of spans is assumed to be five, the length of each span is taken as 50m, the weight is taken as 320 kN/m, the height of each pier is taken as 8m, and the cross-section of each pier is taken as 2.5m by 3m. The over-strength ratio θ is calculated (Design Specifications of Highway Bridges, 1998; Karim and Yamazaki, 2003) as 1.21. Now, knowing the height of the pier as 8m and θ as 1.21, the fragility curve parameters λ and ξ for different damage ranks with respect to both *PGA* and *PGV* are obtained using the simplified expressions given in **Equations (4)** and **(5)**, and using the regression coefficients given in **Table 2**. λ and ξ is also obtained by performing a series of both nonlinear static pushover and dynamic response analyses.

Table 2. List of the regression coefficients for the fragility curve parameters obtained from the simplified method

Indices	DR	Parameters																	
		λ									ξ								
		$\lambda_h=b_0+b_1h+b_2h^2$					$F_\theta=a_0+a_1\Delta\theta$				$\xi_h=b_0+b_1h+b_2h^2$					$F_\theta=a_0+a_1\Delta\theta$			
		b_0	b_1	b_2	σ	R^2	a_0	a_1	σ	R^2	b_0	b_1	b_2	σ	R^2	a_0	a_1	σ	R^2
PGA	S	6.30	0.03	-0.0024	0.022	0.984	1.00	0.11	0.00	1.00	0.40	-0.0006	-0.0006	0.007	0.990	1.00	-0.39	0.00	1.00
	M	6.58	0.01	-0.0005	0.031	0.812	1.00	0.10	0.00	1.00	0.41	0.0002	0.0001	0.012	0.981	1.00	-0.38	0.00	1.00
	E	6.67	0.02	-0.0010	0.017	0.906	1.00	0.10	0.00	1.00	0.27	-0.0008	0.0003	0.015	0.971	1.00	-0.63	0.00	1.00
	C	7.02	-0.02	0.0003	0.047	0.770	1.00	0.10	0.00	1.00	0.38	-0.0043	0.0002	0.002	0.997	1.00	-0.70	0.00	1.00
PGV	S	4.42	0.001	-0.002	0.013	0.998	1.00	0.31	0.00	1.00	0.59	-0.001	-0.0002	0.007	0.967	1.00	0.24	0.00	1.00
	M	4.25	0.091	-0.004	0.036	0.933	1.00	0.26	0.00	1.00	0.59	0.005	-0.0005	0.008	0.978	1.00	0.48	0.00	1.00
	E	4.51	0.080	-0.004	0.016	0.994	1.00	0.29	0.00	1.00	0.63	0.004	-0.0005	0.010	0.969	1.00	0.47	0.00	1.00
	C	489	0.068	-0.003	0.015	0.973	1.00	0.18	0.00	1.00	0.87	-0.034	0.0007	0.011	0.991	1.00	0.67	0.00	1.00

DR: Damage Rank, S: Slight, M: Moderate, E: Extensive, C: Complete.

Table 3. List of the fragility curve parameters for the example isolated bridge structure obtained from the both analytical and simplified methods

Indices	DR	Parameters					
		λ			ξ		
		analytical	simplified	error, ε (%)	analytical	simplified	error, ε (%)
PGA	S	6.60	6.56	0.61	0.52	0.51	1.57
	M	6.82	6.77	0.77	0.47	0.45	3.46
	E	6.94	6.89	0.72	0.42	0.41	2.14
	C	7.14	7.03	1.55	0.42	0.34	19.77
PGV	S	4.60	4.57	0.61	0.59	0.60	1.04
	M	4.96	4.96	0.12	0.63	0.66	3.52
	E	5.26	5.16	1.80	0.75	0.69	7.86
	C	5.46	5.43	0.53	0.75	0.73	3.05

DR: Damage Rank, S: Slight, M: Moderate, E: Extensive, C: Complete.

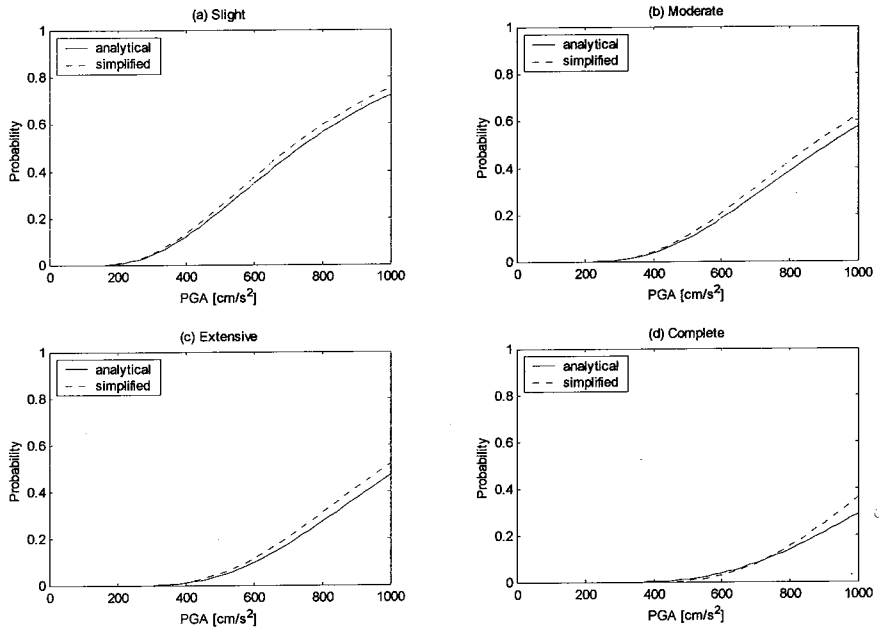

Figure 7. Comparison of the fragility curves obtained from the both analytical and simplified methods for an isolated bridge system with respect to *PGA*

Table 3 shows the list of the fragility curve parameters for the example bridge structure obtained from the both analytical and simplified methods, and the corresponding errors ε for the both λ and ξ with respect to the analytical ones are also shown in the same **Table**. **Figures 7** and **8** show the

fragility curves for the all damage ranks with respect to *PGA* and *PGV*, respectively, obtained from the both analytical and simplified methods. It can be seen that the fragility curves obtained by the both analytical and simplified methods seem to be very close with respect to *PGV*, however, a very small difference is observed with respect to *PGA* for the all damage ranks. Note that the maximum error with respect to both *PGA* and *PGV* for both λ and ξ are shown in **Table 3** with an underline mark. It can be seen that the maximum error for λ with respect to both *PGA* and *PGV* is found to be only 1.8%, and for ξ, it is found as 19.8%.

It should be noted that λ controls the amplitude and ξ controls the shape of the fragility curves. The 19.8% error for ξ does not necessarily mean that it might result a significant effect on the fragility curves, and the evidence can be seen in the fragility curves (**Figures 7 and 8**). Hence, the error terms for both λ and ξ given in **Table 3** seem to be within an acceptable range, and the simplified method may conveniently be used to construct the fragility curves for isolated bridge structures knowing the height h and over-strength ratio θ only. It should be noted that the simplified expressions of fragility curve parameters are obtained based on a set of isolated bridge systems, and these simplified expressions for fragility curve parameters may conveniently be used to construct the fragility curves of similar kind of isolated bridge structures that fall within the same group and have similar characteristics.

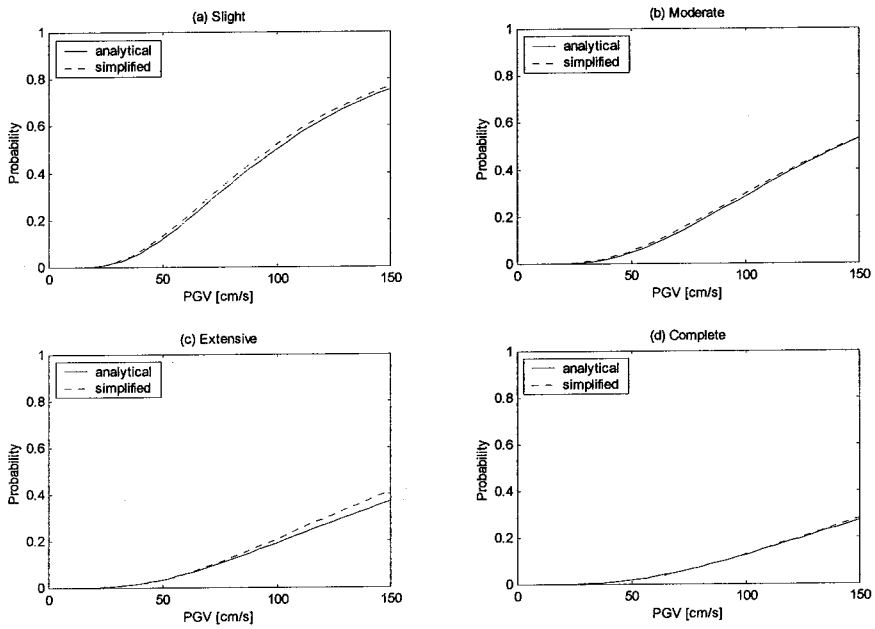

Figure 8. Comparison of the fragility curves obtained from the both analytical and simplified methods for an isolated bridge system with respect to *PGV*

FRAGILITY CURVES FOR THE BOTH ISOLATED AND NON-ISOLATED BRIDGES

The present authors (Karim and Yamazaki, 2003) also developed simplified expressions to construct fragility curves of non-isolated highway bridges. In this study, following the same procedure, simplified expressions are also developed to construct the fragility curves for isolated highway bridges, which are given in the preceding section. Since simplified expressions show the correlation between

the fragility curve parameters and the structural parameters, they might conveniently be used to construct the fragility curves for the both isolated and non-isolated bridges. However, since the two systems are different, it is necessary to see how the fragility curves of the both systems differ from each other based on the simplified expressions.

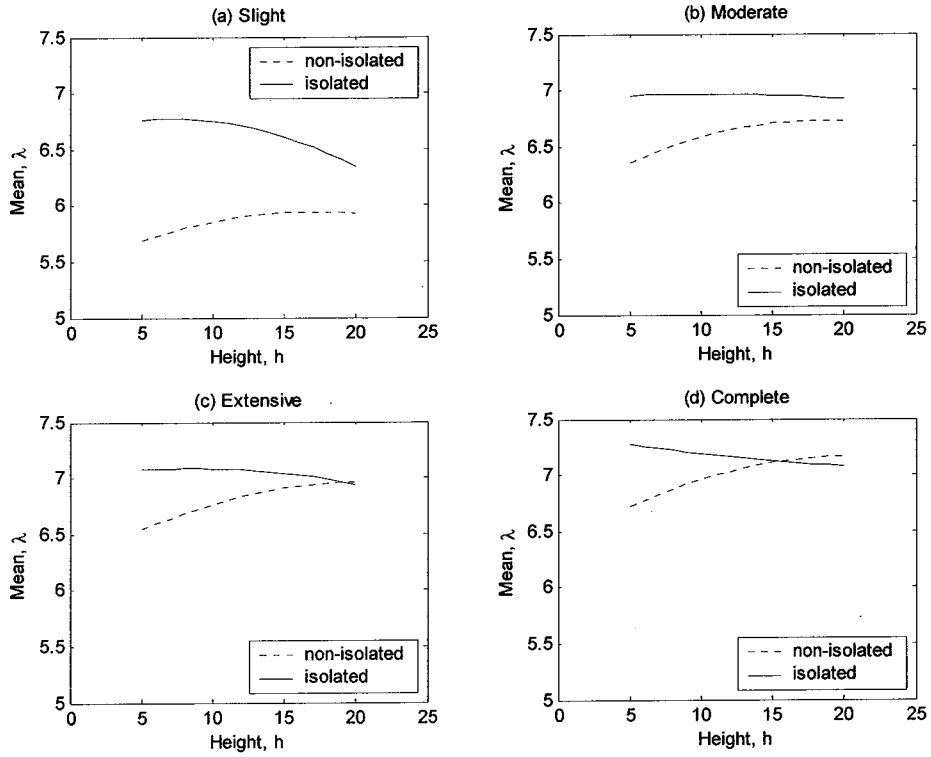

Figure 9. Comparison of the relationship between λ and h for a θ equal to 1.5 obtained from the simplified method for the isolated and non-isolated bridge systems for different damage ranks with respect to *PGA*

Figure 9 shows the plots of the relationship between fragility curve parameter mean λ and pier height h for a θ equal to 1.5 obtained from the simplified method for the both isolated and non-isolated systems for different damage ranks with respect to *PGA*. Note that the simplified expressions for the non-isolated system were taken from the previous study (Karim and Yamazaki, 2003). It can be seen that the λ for the isolated system is higher than that of the non-isolated one for the all damage ranks for a lower level of pier height, which implies that the level of damage probability for the isolated system is less than that of the non-isolated one when the level of pier height is not so large. However, one can see that as the pier height changes from lower to a higher level, the mean λ of the isolated system seems to get closer to the non-isolated one, and eventually, in case of extensive and complete damages, it is less than that of the non-isolated one after a certain level of pier height. Similar trend is also found with respect to *PGV*, and the plots are shown in **Figure 10**.

The trend of converging the mean λ of the isolated system with that of the non-isolated one for a higher level of pier height implies that if the pier height of the bridge is very high, for instance, say more than 20m, then the isolated system may not be so effective. It should be noted that fragility curves are also a function of standard deviation ξ, and the both mean λ and standard deviation ξ are

also a function of scale factor F_θ that is obtained for a given over-strength ratio θ. Hence, to see the effect of isolation on fragility curves, it is necessary to construct them for the both isolated and non-isolated systems considering all these factors.

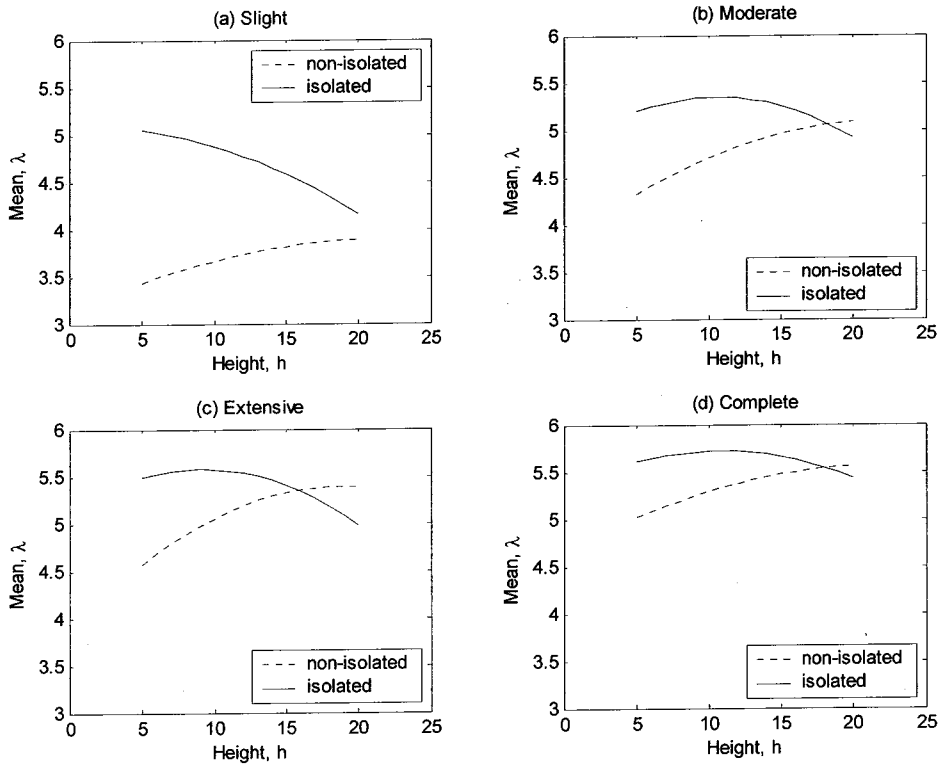

Figure 10. Comparison of the relationship between λ and h for a θ equal to 1.5 obtained from the simplified method for the isolated and non-isolated bridge systems for different damage ranks with respect to *PGV*

Figure 11 shows the plots of the fragility curves for the isolated and non-isolated bridges for an extensive damage with respect to *PGA* obtained from the simplified expressions for different level of pier heights with an over-strength ratio θ equal to 1.5. It can be seen (**Figures 11(a)** and **(b)**) that the level of damage probability for the isolated system is less than that of the non-isolated one for a pier height of 5m and 10m, respectively, and its damage level seems to be similar to that of the non-isolated one when the pier height is 15m (**Figure 11 (c)**). Now, if one looks at **Figure 11 (d)**, then it can be seen that the level of damage probability for the isolated system is higher than that of the non-isolated one where the pier height is 20m. Similar trend is also observed on the fragility curves obtained for the both isolated and non-isolated systems with respect to *PGV*, and the plots are shown in **Figure 12**. Note that the over-strength ratio θ is considered being the same for all levels of pier heights, and it is taken as 1.5. It means that when the pier height is to be higher then even having the same over-strength ratio, the level of damage probability for the isolated system goes higher compared to the one of the non-isolated system.

Although, the soil-structure interaction (SSI) effect is generally not so severe for non-isolated bridge structures except for the case with strong soil non-linearity. However, isolated bridges are regarded to be more susceptible to the effect of SSI during an earthquake (Chaudhary *et al.*, 2001). Thus, it is

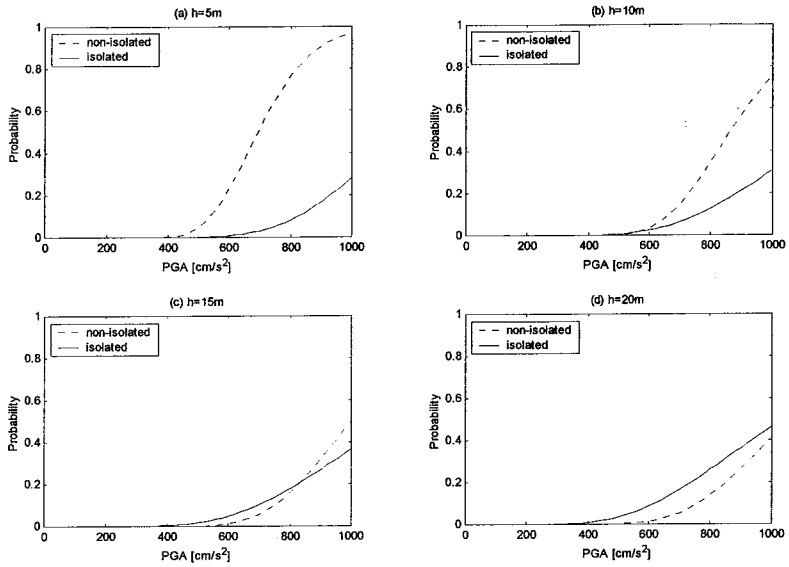

Figure 11. Comparison of the fragility curves for the isolated and non-isolated bridge systems with respect to *PGA* obtained from the simplified method for different pier heights, all for an extensive damage with a θ equal to 1.5

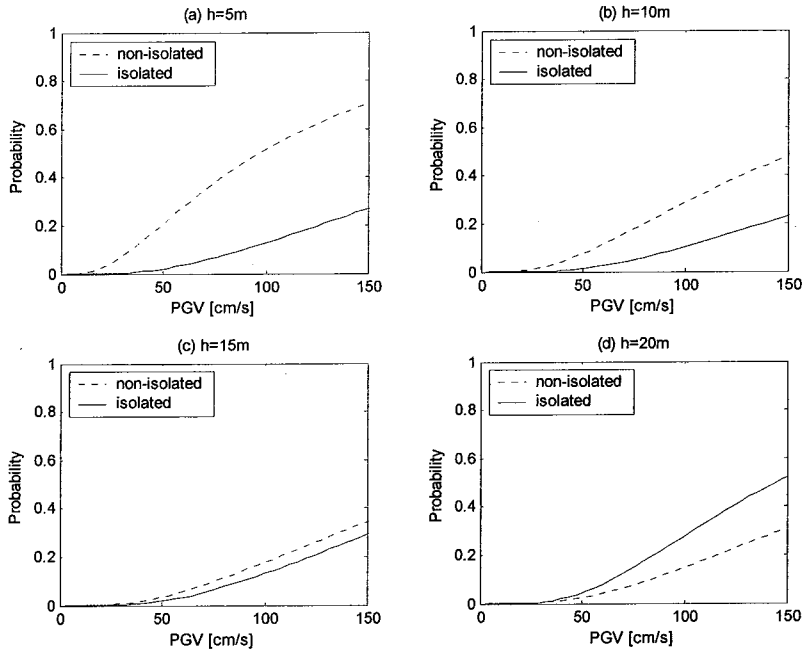

Figure 12. Comparison of the fragility curves for the isolated and non-isolated bridge systems with respect to *PGV* obtained from the simplified method for different pier heights, all for an extensive damage with a θ equal to 1.5

anticipated that there might be an effect on the fragility curves of isolated bridges due to SSI; hence, a further research is necessary in this regard.

CONCLUSIONS

Simplified expressions of fragility curve parameters for isolated highway bridge structures were obtained based on numerical simulation with respect to the ground motion parameters using two hundred and fifty strong motion records. The simplified expressions may be a very useful tool, and conveniently be used to construct the fragility curves for isolated bridges that fall within the same group and have similar characteristics.

Fragility curves for the both isolated and non-isolated systems were also constructed based on the obtained simplified expressions. It was observed that the level of damage probability for the isolated system is less than that of the non-isolated one for a lower level of pier height. However, having the same over-strength ratio of the bridges, the level of damage probability for the isolated system is found to be higher for a higher level of pier height compared to the one of the non-isolated system. It implies that the level of damage probability for the isolated systems tends to be higher for a higher level of pier height.

It is anticipated that the simplified expressions of fragility curves developed in this study may not be applicable for the isolated systems that have SSI effect, and a further research is recommended on this matter.

REFERENCES

Basoz, N. and Kiremidjian, A. S. (1997). "Evaluation of bridge damage data from the Loma Prieta and Northridge, CA Earthquakes." *Report No. 127*, The John A. Blume Earthquake Engineering Center, Department of Civil Engineering, Stanford University.

Bentz, E. C. and Collins, M. P. (2000). "Response-2000." *Software Program for Load-Deformation Response of Reinforced Concrete Section*, http://www.ecf.utoronto.ca/~ bentz/inter4/inter4.shtml.

Chaudhary, M. T. A., Abe, M., Fujino, Y. and Yoshida, J. (2000). "System identification and performance evaluation of two base-isolated bridges using seismic data." *Journal of Structural Engineering*, ASCE, Vol. 126, No. 10, 1187-1196.

Chaudhary, M. T. A., Abe, M. and Fujino, Y. (2001). "Identification of soil-structure interaction effect in base-isolated bridges from earthquake records." *Soil Dynamics and Earthquake Engineering*, Vol. 21, No. 8, 713-725.

Chopra, A. K. (1995). *Dynamics of Structures*: *Theory and Application to Earthquake Engineering*, Prentice-Hall, Upper Saddle River, NJ, USA.

Design Specifications of Highway Bridges (1998). "Part V: seismic design." *Technical Memorandum of EED*, PWRI, No. 9801.

Ghobarah, A. and Ali, H. M. (1988). "Seismic performance of highway bridges." *Engineering Structure*, Vol. 10, 157-166.

Ghobarah, A., Aly, N. M. and El-Attar, M. (1997). "Performance level criteria and evaluation." *Proceedings of the International Workshop on Seismic Design Methodologies for the next Generation of Codes*, Balkema, Rotterdam, 207-215.

Karim, K. R. and Yamazaki, F. (2001). "Effect of earthquake ground motions on fragility curves of highway bridge piers based on numerical simulation." *Earthquake Engineering and Structural Dynamics*, Vol. 30, No. 12, 1839-1856.

Karim, K.R. and Yamazaki, F. (2003). "A simplified method of constructing fragility curves for highway bridges." *Earthquake Engineering and Structural Dynamics* (in press).

Kawashima, K. and Macrae, G. A. (1993). "The seismic response of bilinear oscillators using Japanese earthquake records." *Journal of Research*, PWRI, Ministry of Construction, Japan, Vol. 30, 7-146.

Kawashima, K. and Shoji, G. (1998). "Interaction of hysteretic behavior between isolator/damper and

pier in an isolated bridge." *Journal of Structural Engineering*, JSCE, Vol. 44A, 213-221.
Kircher, C. A., Nassar, A. A., Kustu, O. and Holmes, W. T. (1997). "Development of building damage functions for earthquake loss estimation." *Earthquake Spectra*, Vol. 13, No. 4, 663-682.
Mander, J. B. and Basoz, N. (1999). "Seismic fragility curves theory for highway bridges." *Proceedings of the 5th U.S. Conference on Lifeline Earthquake Engineering*, TCLEE No. 16, ASCE, 31-40.
Park, Y. J. and Ang, A.H-S. (1985). "Seismic damage analysis of reinforced concrete buildings." *Journal of Structural Engineering*, ASCE, Vol. 111, No. 4, 740-757.
Priestley, M. J. N., Seible, F. and Calvi, G. M. (1996). *Seismic Design and Retrofit of Bridges*, Wiley, New York, USA.
SAP2000 (2000). *Integrated Structural Analysis and Design Software*, Computers & Structures Inc.
Sucuoglu, H., Yucemen, S., Gezer, A. and Erberik, A. (1999). "Statistical evaluation of the damage potential of earthquake ground motions." *Structural Safety*, Vol. 20, No. 4, 357-378.
Uang, C-M. and Bertero, V. V. (1990). "Evaluation of seismic energy in structures." *Earthquake Engineering and Structural Dynamics*, Vol. 19, 77-90.
Yamazaki, F., Motomura, H. and Hamada T. (2000). "Damage assessment of expressway networks in Japan based on seismic monitoring." *12th World Conference on Earthquake Engineering*, CD-ROM, Paper No. 0551.